Investigating lipid transporter protein and lipid interactions using variable temperature electrospray ionization, ultraviolet photodissociation mass spectrometry, and collision cross section analysis

Virginia K. James[1], Bradley J. Voss[2], Amanda Helms[1], M. Stephen Trent[2,3], Jennifer S. Brodbelt[1]*

1. Department of Chemistry, The University of Texas at Austin, Austin, TX 78712
2. Department of Infectious Diseases, College of Veterinary Medicine, University of Georgia, Athens, Georgia, USA
3. Department of Microbiology, College of Arts and Sciences, University of Georgia, Athens, Georgia, USA

*Correspondence: jbrodbelt@cm.utexas.edu

Abstract: Gram-negative bacteria develop and exhibit resistance to antibiotics owing to their highly asymmetric outer membrane maintained by a group of six proteins comprising the Mla (maintenance of lipid asymmetry) pathway. Here we investigate the lipid binding preferences of one Mla protein, MlaC, which transports lipids through the periplasm. We used ultraviolet photodissociation (UVPD) to identify and characterize modifications of lipids endogenously bound to MlaC expressed in three different bacteria strains. UVPD was also used to localize lipid binding to MlaC residues 130-140, consistent with the crystal structure reported for lipid-bound MlaC. The impact of removing the bound lipid from MlaC on its structure was monitored based on collision cross section (CCS) measurements, revealing that the protein unfolded prior to release of the lipid. The lipid selectivity of MlaC was evaluated based on titrimetric experiments, indicating that MlaC bound lipids in various classes (sphingolipids, glycerophospholipids, fatty acids) as long as they possessed no more than two acyl chains.

Introduction

While bacteria are relatively well-understood organisms, bacterial infections still account for over 13% of global deaths annually.[1] The number of bacterial infections continues to increase with the rise of antibiotic resistance,[2,3] and by the year 2050, it is estimated that bacterial infections will cause 10 million deaths per year.[4] Gram-negative bacteria often cause the most deadly infections as these bacteria are resistant to more classes and types of antibiotics.[5] Gram-negative bacteria have a unique outer cellular membrane (OM) which is assembled asymmetrically with lipopolysaccharides (LPS) that thwart cellular entry of antibiotics.[6,7] Construction of this asymmetrical OM is governed by the LPS transport pathway that facilitates transport of LPS to the OM.[8] While the LPS are the key unique feature of the OM, glycerophospholipids (GPLs) are also needed to maintain the inner membrane, the periplasmic side of the OM, and short segments of the extracellular side of the OM. However, if excessive GPLs accumulate in the extracellular side of the OM, the OM becomes more susceptible to permeation by small molecules like antibiotics.[9] A system of proteins, known as the maintenance of lipid asymmetry (Mla), are tasked with removing misplaced GPLs from the extracellular side of the OM to maintain its asymmetry.[10]

The Mla system consists of six proteins designated MlaA-MlaF, and these proteins span from the OM to the cytoplasmic side of the inner membrane. MlaA is embedded in the OM and passes misplaced GPLs to MlaC, a periplasmic protein.[11,12] MlaC then transfers the GPLs to the MlaD-F complex[13] to send the GPLs to the inner membrane where GPLs are reinserted (retrograde).[14,15] Previous work indicated that the Mla system may be able to move GPLs in the reverse direction, *i.e.* transporting GPLs to the outer membrane (anterograde)[16,17]; however, other and more recent work provides substantial evidence that the Mla pathway only functions in retrograde.[11,18–24] A recent study showed that electrostatic interactions between MlaA and MlaC only occur when MlaC is in an apo state, further confirming the retrograde function of the Mla pathway.[25] While MlaA and the MlaD-F complex contain transmembrane domains making them difficult to analyze by many methods owing to solubility issues,[14] MlaC is soluble in aqueous solvents which, along with its small size of 23 kDa and that it typically binds and transports only one lipid at a time,[26] makes the protein more readily characterized.[27] As MlaC is a critical component of the Mla system, examining the lipid binding preferences of MlaC, its conformational changes, and nature of its lipid binding interactions may result in a better understanding of the function of the Mla system as a whole.

Molecular docking and other computational methods have shown that MlaC interacts with the hydrophobic acyl chains of GPLs, [28] unlike many proteins with transmembrane domains which can interact

with both the lipid headgroup and acyl chain depending on the hydrophobicity in that region of the protein.[29,30] Given that MlaC is thought to be a transporter protein that shuttles lipids between MlaA and MlaDEBF complex, this binding orientation is logical given that the proposed lipid transfer through the Mla system involves the polar lipid headgroup disassociating from MlaA last and then interacting with the MlaDEBF complex via the headgroup first.[23] MlaC has been shown to bind GPLs via the acyl chains in *E. coli* as documented in multiple x-ray crystal structures.[17,31] A similar acyl chain-mediated binding configuration was reported for *P. aeruginosa* MlaC, but this MlaC species had a sufficiently large binding cavity to accommodate two GPLs at once as determined by x-ray crystallography (PBD 6HSY), indicating that *P. aeruginosa* may use the Mla system to transport larger lipids that contain more than two acyl chains such as cardiolipin.[26]

Advanced mass spectrometry methods have increasingly been developed and applied to decipher stoichiometries, structures, interactions, and topologies of protein-ligand complexes.[30,32,33] To probe lipid binding preferences, mass spectrometry has been used to identify lipids washed from MlaC or dislodged from MlaC under denaturing conditions.[16,26] Primarily GPLs[16] and possible partial structures of cardiolipins[26] were found, all common in Gram-negative bacteria.[34] Further, native mass spectrometry (native MS), a strategy which entails using electrospray ionization (ESI) of aqueous solutions of high ionic strength to preserve native-like protein structures, was employed to examine intact MlaC●lipid complexes from *P. aeruginosa*.[26] Native mass spectrometry was used to support x-ray crystallography data that suggested that MlaC from *P. aeruginosa* could be bound to two GPLs at once and/or one cardiolipin,[26] although the mass resolution was insufficient for definitive claims. Deeper characterization of protein-ligand interactions has been achieved by using high resolution native mass spectrometry,[35] allowing even small mass shifts in bound ligands corresponding to a single lipid saturation to be resolved. Further, tandem MS, particularly ultraviolet photodissociation (UVPD), has been employed to localize lipid binding to membrane proteins.[36] UVPD, a higher energy activation technique, induces backbone cleavages while maintaining the integrity of non-covalent protein-ligand interactions, thus allowing the localization of ligands through the generation of holo (ligand-retaining) fragment ions.[37–39] Moreover, UVPD of individual lipids provides extensive structural information such as the identification and localization of unsaturation elements,[40,41] features that are difficult to discern by conventional MS/MS methods. Auxiliary mass spectrometry techniques such variable temperature ESI have been used to evaluate the stabilities and thermodynamic parameters of membrane proteins and their lipid complexes,[42,43] and collision cross section (CCS) measurements have revealed conformational changes of membrane proteins upon lipid binding.[44,45]

Owing to its lack of a transmembrane domain and therefore solubility in aqueous solvents without adducts, MlaC presents a unique opportunity to study the effects of collisional activation on retention of native protein structure. Although membrane protein titration experiments[46] have revealed lipid binding preferences of membrane proteins,[47,48] endogenously bound lipids are rarely characterized owing to spectral complexity as many membrane proteins bind multiple lipid species at once.[48] Herein, we use native mass spectrometry to characterize the conformational size of MlaC without and with bound lipids via collision cross section measurements, to localize the lipid binding site and the identity of endogenously bound lipids by UVPD, and determine lipid binding preferences based on variable temperature and titrimetric experiments.

Experimental

Materials

Equine heart myoglobin and ammonium acetate were purchased from Sigma-Aldrich (St. Louis, MO, USA). LC-MS grade water and methanol was purchased from Merck Millipore (Billerica, MA, USA). Octyl glucoside and lipid standards (**Table S1**) were purchased from Cayman Chemicals, except for the cardiolipin, which was purchased from Avanti Polar Lipids. For non-denaturing experiments, proteins were diluted in 100 mM ammonium acetate to a final concentration of 10 µM. For denaturing experiments proteins were diluted to 20 µM in 0.1% formic acid and desalted with Micro Bio-Spin™ P-6 Gel Columns (Bio-Rad Laboratories Inc., Hercules, CA) three times to remove excess glycerol, then diluted with methanol to a final concentration of 10 µM.

Plasmid and strain construction

For expression of MlaC in W3110, endogenous *mlaC* was deleted via P1 transduction of *mlaC*::kan from BW25113 *mlaC*::kan (Keio Collection). The kanamycin (kan) resistance cassette was removed by transformation with temperature instable *pCP20*. After kan cassette excision, *pCP20* was cured by incubation at 42 ^{O}C overnight. Resulting strain was named W3110Δ*mlaC.*

pQLinkN was used in the expression of MlaC-His_8 in W3110 Δ*mlaC*. Prior to inserting *mlaC* into *pQLinkN* the chloramphenicol acetyltransferase was removed from the vector using NheI and NcoI restriction sites, blunted with Klenow large fragment, and circularized using blunt-end ligation. Resulting vector was named *pQLink*. *mlaC-His_8* was amplified from W3110 using primers encoding BamHI and NotI restriction site overhangs, and carboxy-terminal poly-histidine tag (**Table S2**) and ligated into *pQLink* to produce *pQLink-*

mlaC-His$_8$. The plasmid was then transformed into W3110Δ*mlaC* using electroporation for protein expression.

pET21a was used in the expression of MlaC-His$_8$ in HMS174(DE3) and C43(DE3). *mlaC-His$_8$* was amplified from W3110 using primers encoding NdeI and BamHI restriction site overhangs, and carboxy-terminal poly-histidine tag (**Table S2**) and ligated into *pET21a* to produce *pET21-mlaC-His$_8$*. Plasmid was transformed into HMS174(DE3) using electroporation and chemically competent C43(DE3) using heat shock transformation.

Protein expression

MlaC was expressed and purified in house in three different strains of bacteria including W3110 (a wild-type standard *E. coli* K-12 strain), HMS174(DE3) (a K-12 strain harboring the DE3 lysogen allowing for pET-based overexpression), and *E. coli* strain C43(DE3). MlaC-His$_8$ was expressed from *pET21-mlaC-His$_8$* for strains HMS174(DE3) and C43(DE3) and *pQLink-mlaC-His$_8$* for W3110Δ*mlaC*. For HMS174, and W3110Δ*mlaC*, 1 L cultures were subcultured 1:100 from overnight culture. For C43(DE3) *pET21-mlaC-His$_8$*, 500 mL LB culture was subcultured 1:100 from overnight culture. For all strains, after two hours of subculture growth at 37 ^{O}C, MlaC-His$_8$ was induced with the addition of IPTG to 1 mM final concentration. After four hours of induction, bacteria were harvested, washed in PBS, and resuspended at 100 mg wet pellet/mL lysis buffer (50 mM HEPES pH 7.5, 500 mM NaCl, 40 mM Imidazole, 10% Glycerol). 1 mg/mL lysozyme and 50 U/mL benzonase were added to the bacterial suspension and lysed with a French Press at 20,000 PSI. EDTA-free protease inhibitor cocktail (Sigma) was added to 1x final concentration. Cellular debris was removed by centrifugation at 5,000 x g for 15 minutes. Membranes were removed from the lysate by centrifugation at 100,000 x g for 1 hour. MlaC-His$_8$ was purified using HisTrap FF (Cytiva) and eluted with a linear gradient of lysis buffer containing 500 mM Imidazole. Elution fractions containing MlaC-His$_8$ were concentrated using Vivaspin 10,000 Da cutoff spin column (Cytiva) and MlaC-His$_8$ was further resolved using Supderdex 200 Increase 10/30 GL size exclusion (Cytiva). MlaC-His$_8$ containing fractions were concentrated using Vivaspin 10,000 Da spin column. Protein concentrations were determined using Pierce BCA protein assay kit (Thermo).

The MlaC sequence is given in **Table S3**, and more details about samples from each strain are shown in **Table S4**. MS1 and sequence maps generated from MS/MS spectra of each MlaC protein are included in **Figure S1-S3**.

Lipid Titration

Lipid titration experiments were performed as previously described.[46] Briefly, octyl glucoside was added to a 20 µM sample of MlaC in a solution comprised of 50 mM HEPES pH 7.5, 500 mM NaCl, and 10% glycerol to reach a final concentration of 1% octyl glucoside. The sample was incubated with 1% octyl glucoside overnight at room temperature, which allowed significant delipidation without protein degradation. The sample was buffer exchanged three times as described above to remove the detergent and excess glycerol. Exogenous lipids were then added from methanol stock solutions, giving a ratio of 1:10 protein to lipid and less than 1% methanol. Gentle heating (37 °C) or sonication was used for up to 1 hour to enhance protein-lipid binding.

Instrumentation

All experiments were performed on a Thermo Scientific™ Q Exactive™ HF-X quadrupole-Orbitrap mass spectrometer (Bremen, Germany) with Biopharma option, which was modified to collect two-second-long transients, corresponding to a resolution of 960,000 at *m/z* 200, necessary to calculate CCS. A 500 Hz, 193 nm Coherent® ExciStar excimer laser (Santa Cruz, CA) was interfaced as previously described to perform UVPD in the HCD cell.[49,50] Ions were generated by nano-ESI ionization using Au/Pt-coated borosilicate emitters fabricated in-house and using a spray voltage of 0.8-1.6 kV. For variable temperature experiments, a variable temperature ESI source was used to modulate the solution temperature during ESI as previously described.[51,52] CCS measurements of MlaC (9+ charge state) were undertaken after stepwise in-source collisional activation and isolation in the quadrupole using an isolation width of 5-10 *m/z* at a resolution of 960,000. Low resolution (7,500) MS1 spectra were also monitored during stepwise in-source collisional activation to determine the fractional abundance of lipid bound species. For UVPD experiments, MlaC lipid complexes (9+ charge state) were mass-selected in the quadrupole with an isolation width of 5-10 *m/z,* and spectra were collected at 240,000 resolution, using 250 averages per replicate. For endogenous lipid identifications, a pseudo MS^3 method with in-source collision activation was used to release lipids from the protein-lipid complexes, followed by UVPD of each lipid species in the negative mode. The C-trap gas pressure was set to 1 for all experiments, corresponding to a UHV gauge reading of around 1E-10 to 1.5E-10 mbar, respectively. All data was collected with high mass range (HMR) mode on and default ion optic voltages.

Data Acquisition and Processing

A custom license provided by Thermo Fisher Scientific allowed the collection of transient data needed for CCS measurements. Transients were processed using the direct decay profile fitting method

with a custom MATLAB R2020a script as previously described.[53,54] All CCS data were calibrated to myoglobin (8+ charge state, ion mobility CCS 1966 Å^2) collected at the same pressure and on the same day, and CCSs were fitted owing to extended ion survival as previously described.[55] Variable temperature ESI data was analyzed using a custom MATLAB R2020a script as previously described.[51] All CCS and variable temperature ESI data were collected in triplicate, and error bars represent the standard deviation of these replicates. UVPD spectra were deconvoluted using Xtract in QualBrowser, and sequence coverage maps were generated from the deconvoluted data using MS-TAFI with a 10 ppm error tolerance.[56] MS-TAFI was used to compare UVPD replicate data so that only fragment ions identified in at least two out of three replicates were retained. Prosight Native was used to confirm isotopic distributions of holo ions identified in UVPD mass spectra acquired for MlaC•lipid ions.[57] Unidec was used for the deconvolution of low-resolution data to calculate fractional abundance of lipid bound species.[58,59] Ejected endogenously bound lipids were identified by comparing their UVPD fragmentation to theoretical fragmentation patterns from the LIPID Metabolites and Pathways Strategy structure database (LIPID MAPS, www.lipidmaps.org). Crystal structures were prepared using PyMol (PyMOL Molecular Graphics System, version 2.4 Schrödinger, LLC).

Results and discussion

MlaC endogenously bound lipid preferences varies based on expression strain

To better understand the lipid binding preferences of the Mla system, we first sought to characterize endogenous lipids bound to MlaC. As native mass spectrometry maintains proteins in their native state and uses gentle conditions to transfer proteins to the gas phase, non-covalent lipid binding interactions are preserved. We expressed MlaC in three *E. coli* strains (details **Table S4**), and the MS1 spectra obtained for MlaC derived from each strain are shown in **Figure 1a** (with expanded *m/z* range shown in **Figure S4**) indicating high abundances of 1:1 MlaC•lipid complexes and lower abundances of apo MlaC. In-source collisional activation, a method used to collisionally heat ions, was used to disassemble the MlaC•lipid complexes and release the lipids. Accurate mass measurements of the released lipids were used to identify the lipids bound to MlaC, and typical lipid profiles are shown in **Figure S5** for MlaC derived from the C43 and W3 strains. The presence of free isobaric/isomeric lipids in the low *m/z* region prior to in-source collisional activation would complicate the identification of the bound lipids released from MlaC, but there was no direct evidence of this concern based on examination of the distribution of lipids prior to and after the use of in-source collisional activation (**Figure S6**). MlaC from the C43 strain exhibits a different profile of lipids from the W3 strain, and the mass of the most abundant lipid (*m/z* 702.51) is congruent with an unsaturated

lipid containing one odd-carbon acyl chain, indicative of a cyclopropane modification. UVPD of this lipid yields an informative fragmentation pattern consistent with PE(16:0_17:1), confirmed by a pair of diagnostic fragments (Δ14 Da) characteristic of a cyclopropane moiety (**Figure 1b**). This result substantiates that MlaC expressed in C43 cells primarily binds the highly abundant cyclopropane-containing PE(16:0_17:1).

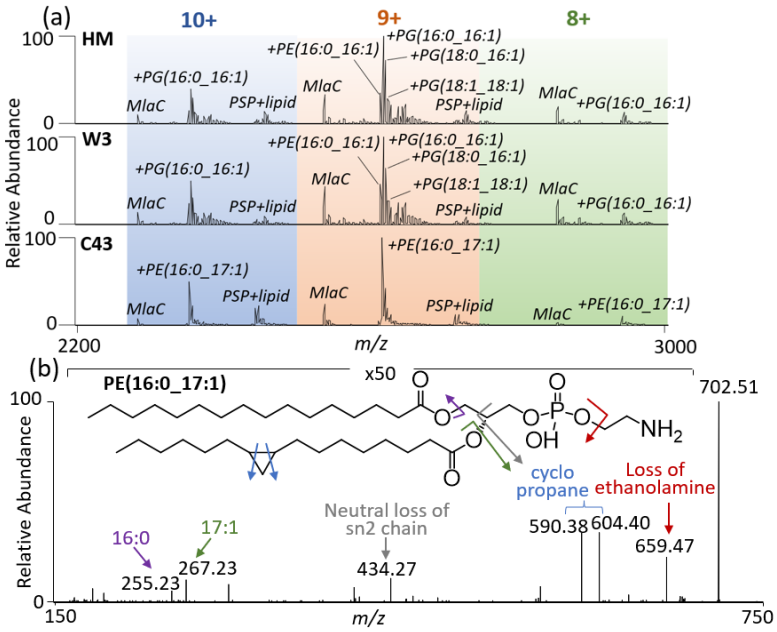

Figure 1. (a) MS1 spectra of MlaC produced in each bacteria strain with the major endogenous bound lipids identified. PSP denotes the MlaC protein with retention of the partial signal peptide. MS1 spectra spanning a broader *m/z* range are shown in **Figure S4**. (b) UVPD mass spectrum (7 pulses, 2.5 mJ per pulse) of the lipid (*m/z* 702.51) released upon in-source collisional activation from the dominant MlaC•lipid complex observed from the C43 strain. The UVPD mass spectra of other lipids bound to MlaC for the HM and W3 strains are shown in **Figure S7.**

UVPD was used to characterize the most abundant lipids released from MlaC from each strain, revealing an array of unsaturated PE and PG lipids (**Figure S7**). Comparison of the bound lipid profiles reveals that MlaC from the HM and W3 strains have very similar endogenously bound lipids in contrast to MlaC from the C43 strain (**Figure S4**). C43 cells are known to have an increased inner membrane content leading to bunching of the membrane, a cellular modification which is correlated with lipid structural modifications like cyclopropane motifs.[60,61] Therefore, we suspect that MlaC binds the most abundant GPLs within the membrane and does not appear to exhibit significant preference for specific acyl chain modifications for endogenous lipid content present in overexpression systems. Additionally, the MS1 spectra show that MlaC only binds a single lipid at a time, thus confirming the inability of MlaC to bind multiple lipids simultaneously when expressed in *E. coli,* as also noted in a previous study.[26]

MlaC•PG(18:1/18:1) from the W3 strain was characterized by UVPD, yielding numerous sequence ions as well as apo protein ions (**Figure 2a**). The ejected lipid was not detected, an outcome not unsurprising because these lipids are more readily detected as deprotonated species in the negative mode. In contrast, UVPD of MlaC•PE(16:0_16:1) resulted in detection of free PE(16:0_16:1) as a protonated species (**Figure S8**). For the sequence ions produced upon UVPD of the MlaC•lipid complexes, they may be classified as "apo" (the lipid is not retained) or "holo" (the lipid is retained), and the pattern of these ions can be used to localize the general lipid binding site (**Figure 2b**). There are no fragment ions originating from backbone cleavages spanning residues 131-142, a notable difference compared to the rest of the protein (**Figure S9a**), and a few lipid-containing holo fragment ions that encompass this region are detected when fixing the lipid at K133 (**Figure S9b**). Several other possible lipid binding sites were considered (**Figure S10).** Relatively high sequence coverages were also obtained when fixing the lipid at K107, K156 and K167; however, positioning the lipid at K133 gave the highest overall sequence coverage. These observations suggest that the lipid is associated in this region of the protein, consistent with previous X-ray crystallography, cryo-EM, and molecular docking studies of MlaC that have localized binding of the lipid acyl chains as seen in **Figure 2c**.[12,17,26,27,31] The backbone cleavage sites from which the lipid-retaining holo ions produced upon UVPD of MlaC•PG(18:0_16:0) (*e.g.* holo ions) are shaded on the crystal structure in **Figure 2c**.

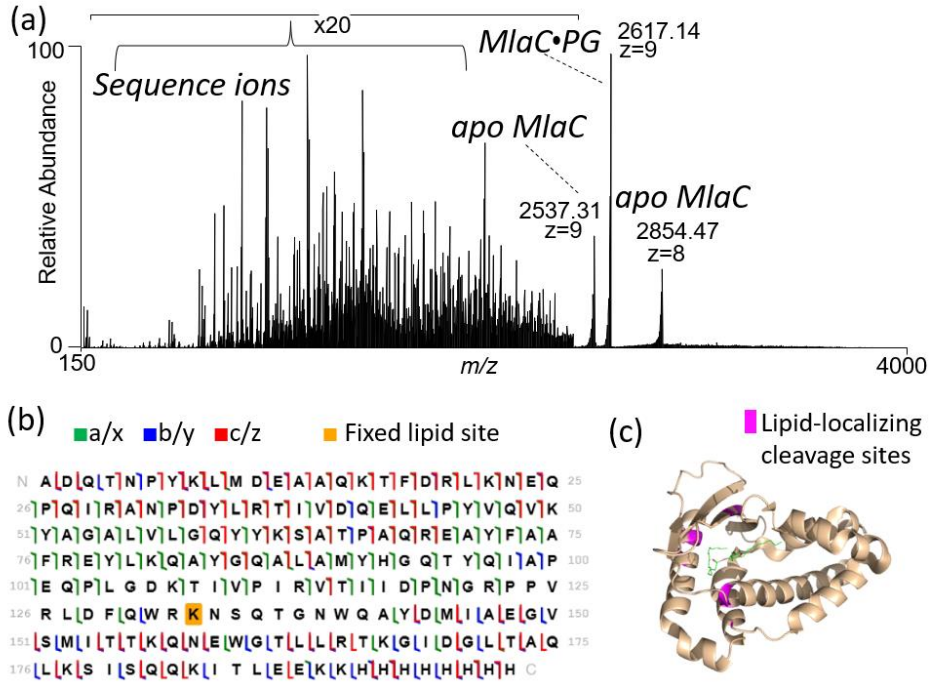

Figure 2. (a) UVPD mass spectrum (1 pulse, 2.5 mJ) of MlaC●PG(18:0_16:0) (9+) and (b) the resulting sequence coverage map generated based on combined apo and holo fragment ions with the lipid fixed at K133 (which offered the highest sequence coverage). Sequence coverages were 76% based on apo fragment ions and 84% when including lipid-bound holo fragment ions. Sequence coverage maps for

MlaC●PG(18:0/16:0) based on apo fragment ions (no lipid bound), holo ions only (lipid bound, fixed at K133), and the combined map are shown in **Figure S9**, and fragment ion identifications are provided in **Supplemental Information (Table S5).** (c) The crystal structure of MlaC (PDB 5UWA with green lipid ((2S)-3-(2-aminoethoxy)propane-1,2-diyl dihexadecanoate); in this structure, some residues (N-terminal residues A1 to D2 and C-terminal residues E187 to H198) were not included in the construct or were not resolved crystallographically but are included in the 198 residues shown in the sequence map in (b). The backbone cleavage sites from which the lipid-containing fragment ions originate are highlighted in fuchsia.

MlaC begins to unfold prior to dissociation of lipid

As MlaC is a soluble periplasmic protein, it represents a unique opportunity to study both the apo and lipid-bound protein. In-source collisional activation is often used to remove adducts from proteins to alleviate dispersion of signal among many heterogeneous forms or to disassemble protein complexes to facilitate analysis of the subunits. Here, we monitored the impact of in-source collisional activation on the distribution of adducts and the retention of the native folded structure based on measurement of collision cross sections. Increasing the voltage used for in-source collisional activation causes detachment of the lipid and other adducts from MlaC and increases the signal-to-noise of apo Mlac by over one order of magnitude (**Figure 3a**). The native structure of MlaC is disrupted at collision voltages beyond ~50 V as evidenced by the increase in collision cross section (CCS) of MlaC from 2300 $Å^2$ (in the absence of collisional heating) to 2700 $Å^2$ (for collision voltages greater than 70 V) (**Figure 3b**). Interestingly, all of the bound lipid is not fully detached until collision voltages surpass 100 V, indicating that MlaC unfolds prior to ejection of all lipids (**Figure 3b**). Performing higher resolution ion mobility measurements would be a compelling strategy to examine the impact of the specific lipid on the variation in collision cross section of the protein•lipid complexes as a function of collision induced unfolding. This type of experiment is better suited to a conventional ion mobility mass spectrometer to monitor the structural transitions of the protein.

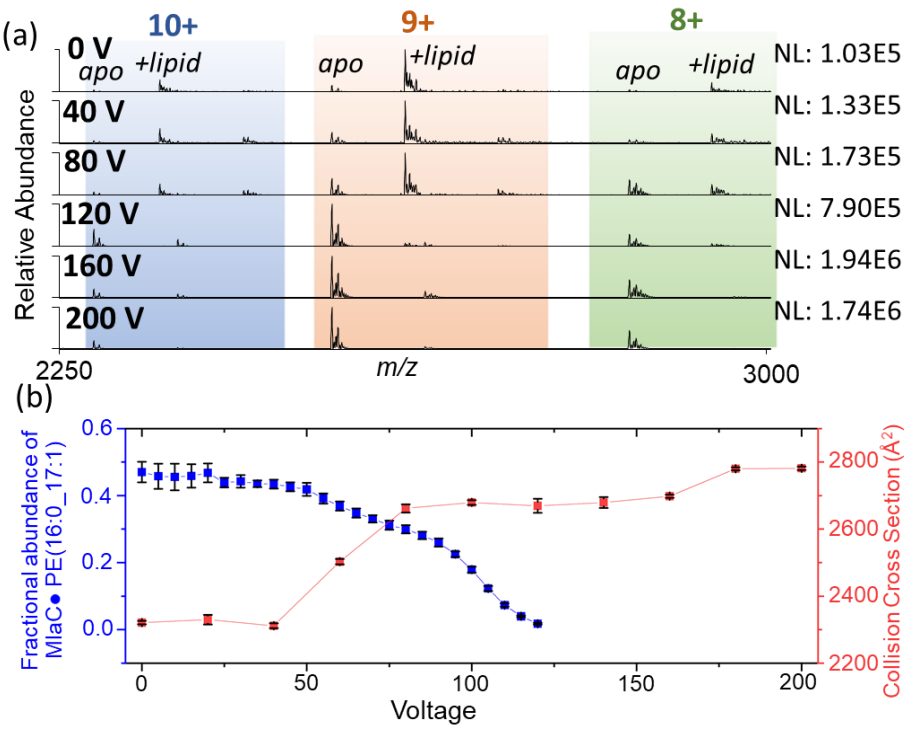

Figure 3. (a) MS1 spectra of MlaC (C43 strain) as a function of the degree of collisional heating via in-source collisional activation. NL represents the normalized level of signal intensity for the spectrum, and larger values indicate higher signal intensity. (b) Fractional abundance of MlaC•PE(16:0_17:1) (relative to the summed abundances of apo MlaC and MlaC•PE(16:0_17:1) and collision cross section of apo MlaC (9+) as a function of collisional heating via in-source collisional activation. Error bars represent the standard deviation based on three replicates.

MlaC binds lipids preferentially based on acyl chain

Understanding the binding preferences of MlaC for exogenous lipids is another key question that provides insight about the selective lipid transport of MlaC in Gram-negative bacteria. A protocol was adapted from previous studies that focused on understanding lipid binding affinities of insoluble proteins with transmembrane domains,[46,62,63] using a detergent to remove all lipids from MlaC prior to re-constitution with other targeted lipids. This method removed approximately 90% of all lipids bound to MlaC, leaving predominantly apo protein (**Figure S11**). A wide array of lipids with differing head groups and number of acyl chains (see **Table S1**) were selected for titration experiments with MlaC. Deconvoluted MS1 spectra obtained for the solutions containing MlaC with each lipid are displayed in **Figure 4**. MlaC binds lipids with different headgroups as long as the lipid has only one or two acyl chains. MlaC even bound a ganglioside, GM1 (d18:1_18:0), a lipid with a very large head group not found in bacteria, suggesting that MlaC binding does not discriminate based on head group but rather based on number of acyl chains. This result is consistent

with the lipid binding and transport pathway proposed for Mla system in which MlaC binds primarily via lipid acyl chains, not by the lipid headgroups engaged by the other Mla proteins.[31] From our earlier identification of endogenously bound lipids, we know that MlaC binds diacyl lipids (**Figure S5**), and we found that MlaC also bound a GPL with only one acyl chain. However, MlaC did not bind lipids that had three or four acyl chains in exogenous lipid binding experiments (**Figure 4b**), an outcome congruent with prior reports of MlaC expressed in *E. coli*.[26,27,31] Collectively these results suggests that Mla only transports mono and diacyl GPLs, not cardiolipin, in *E. coli*. Examination of an even broader array of lipids, such as ones varying in the number and positions of double bonds and lengths of the acyl chains, could provide additional insight into the factors that modulate lipid binding to MlaC.

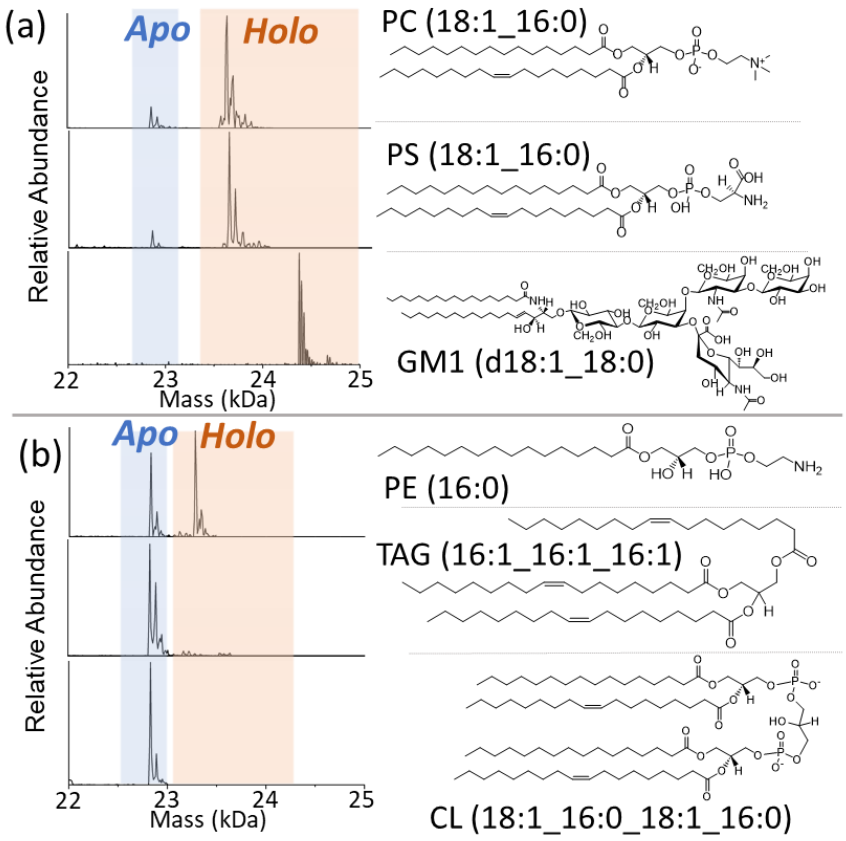

Figure 4. Deconvoluted MS1 spectra obtained for solutions containing MlaC and one lipid. The blue-shaded region corresponds to the apo protein, and the orange-shaded region corresponds to the MlaC•lipid complex. The structures of the lipids are shown based on (a) variation of head group of each lipid and (b) variation of the number of acyl chains.

To further discern differences in lipid binding preferences of MlaC, we used variable temperature ESI to monitor the change in the distribution of MlaC●lipid complexes as a function of solution temperature.

Variable temperature ESI-MS is commonly used to evaluate thermodynamic parameters (based on van't Hoff plots) or unfolding (based on charge state or collision cross section analysis) of protein complexes. Variations in charge state distributions serve as a proxy for protein unfolding because as proteins unfold additional basic residues become accessible, increasing protonation. For MlaC, lipid binding has relatively little impact on the average charge state (Δcharge < 0.2 between apo and holo MlaC) at temperatures ranging from 25-70 °C, and the lipid detaches at approximately 70 °C prior to protein aggregation (80 °C) (**Figure 5**). The similar charge state distributions and average charge states of MlaC and MlaC●lipid over a range of solution temperatures implies that lipid binding does not substantially stabilize the tertiary structure of MlaC and suggests that the conformation of MlaC does not change significantly upon lipid binding. Furthermore, the temperature-dependent charge state distributions of MlaC do not change as a function of the lipid, a trend illustrated in **Figure 5b** that exhibits little change in average charge state across a series of five endogenously bound lipids (**Figure 5b**). This trend further recapitulates that MlaC displays little lipid preference aside from the requirement for one or two acyl chains, although, as noted earlier, there may be yet undiscovered factors related to the number and positions of unsaturation of the acyl chains.

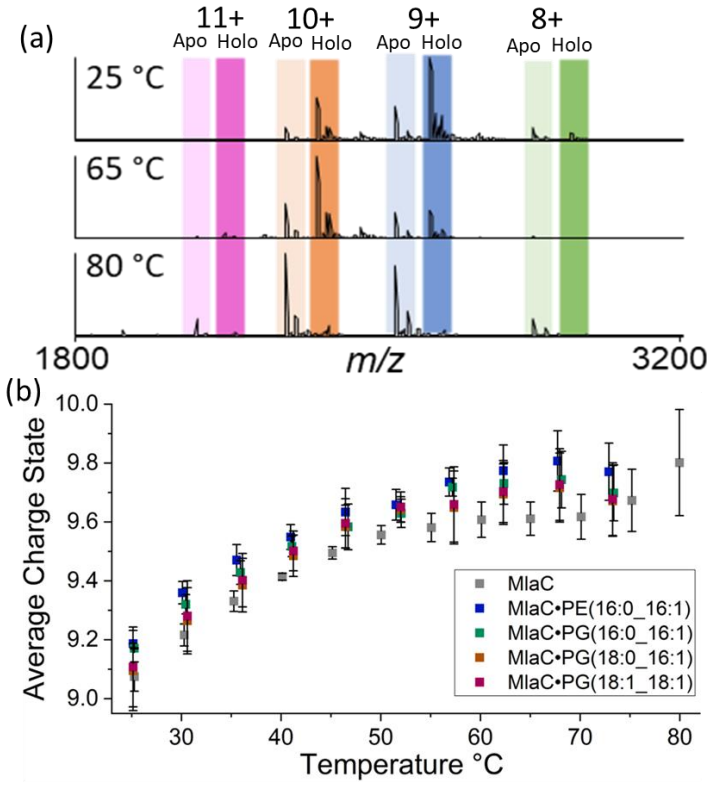

Figure 5. (a) MS1 spectra of solutions containing MlaC with endogenous lipids at 25, 65, and 80 °C, and (b) average charge state of apo MlaC and MlaC•lipid (containing endogenously bound

lipids) as a function of solution temperature. Error bars represent standard deviation from three replicates.

Conclusions:

Using UVPD, we deciphered endogenously bound lipids to the Gram-negative bacteria lipid transporter protein MlaC expressed in different *E.coli* overexpression strains. MlaC produced in C43 strain, known for providing an increased yield of membrane proteins, primarily binds a cyclopropane-containing lipid. MlaC expressed in two other *E. coli* strains preferentially bound saturated lipids and lipids containing double bounds. We also show that collisional activation, commonly used to remove lipids and adducts from membrane proteins, caused the unfolding of MlaC prior to ejection of the lipid. Finally, we show that MlaC exhibits lipid binding preferences based only on acyl chain, as the protein binds a variety of exogenous lipids as long as the lipid has one to two acyl chains. Beyond examination of the Mla system, these methods may be used in future studies to characterize endogenous lipids bound to a variety of lipid transporter proteins and give insight into the lipid binding preferences of proteins produced in overexpression systems.

Supporting Information: Includes structures of lipids, primers for protein expression, sequences of proteins, details about bacterial strains, UVPD spectra and lists of fragment ions, sequence coverage maps, and mass spectra of protein+lipid solutions.

Acknowledgements

Funding from the National Institutes of Health (R35GM13965) and the Robert A. Welch Foundation (F-1155) to J.S.B. is gratefully acknowledged. The Trent group acknowledges funding from the National Institutes of Health, grants R01AI176776, R01AI138576, and R01AI150098 and support from the Army Research Office (ARO) grant W911NF2010195.

References

(1) Ikuta, K. S.; Swetschinski, L. R.; Aguilar, G. R.; Sharara, F.; Mestrovic, T.; Gray, A. P.; Weaver, N. D.; Wool, E. E.; Han, C.; Hayoon, A. G.; Aali, A.; Abate, S. M.; Abbasi-Kangevari, M.; Abbasi-Kangevari, Z.; Abd-Elsalam, S.; Abebe, G.; Abedi, A.; Abhari, A. P.; Abidi, H.; Aboagye, R. G.; Absalan, A.; Ali, H. A.; Acuna, J. M.; Adane, T. D.; Addo, I. Y.; Adegboye, O. A.; Adnan, M.; Adnani, Q. E. S.; Afzal, M. S.; Afzal, S.; Aghdam, Z. B.; Ahinkorah, B. O.; Ahmad, A.; Ahmad, A. R.; Ahmad, R.; Ahmad, S.; Ahmad, S.; Ahmadi, S.; Ahmed, A.; Ahmed, H.; Ahmed, J. Q.; Rashid, T. A.; Ajami, M.; Aji, B.; Akbarzadeh-Khiavi, M.; Akunna, C. J.; Hamad, H. A.; Alahdab, F.; Al-Aly, Z.; Aldeyab, M. A.; Aleman, A. V.; Alhalaiqa, F. A. N.; Alhassan, R. K.; Ali, B. A.; Ali, L.; Ali, S. S.; Alimohamadi, Y.; Alipour, V.; Alizadeh, A.; Aljunid, S. M.; Allel, K.; Almustanyir, S.; Ameyaw, E. K.; Amit, A. M. L.; Anandavelane, N.; Ancuceanu, R.; Andrei, C. L.; Andrei, T.; Anggraini, D.; Ansar, A.; Anyasodor, A. E.; Arabloo, J.; Aravkin, A. Y.; Areda, D.; Aripov, T.; Artamonov, A. A.; Arulappan, J.; Aruleba, R. T.; Asaduzzaman, M.; Ashraf, T.; Athari, S. S.; Atlaw, D.; Attia, S.; Ausloos, M.; Awoke, T.; Quintanilla, B. P. A.; Ayana, T. M.; Azadnajafabad, S.; Jafari, A. A.; B, D. B.; Badar, M.; Badiye, A. D.; Baghcheghi, N.; Bagherieh, S.;

Baig, A. A.; Banerjee, I.; Barac, A.; Bardhan, M.; Barone-Adesi, F.; Barqawi, H. J.; Barrow, A.; Baskaran, P.; Basu, S.; Batiha, A.-M. M.; Bedi, N.; Belete, M. A.; Belgaumi, U. I.; Bender, R. G.; Bhandari, B.; Bhandari, D.; Bhardwaj, P.; Bhaskar, S.; Bhattacharyya, K.; Bhattarai, S.; Bitaraf, S.; Buonsenso, D.; Butt, Z. A.; Santos, F. L. C. dos; Cai, J.; Calina, D.; Camargos, P.; Cámera, L. A.; Cárdenas, R.; Cevik, M.; Chadwick, J.; Charan, J.; Chaurasia, A.; Ching, P. R.; Choudhari, S. G.; Chowdhury, E. K.; Chowdhury, F. R.; Chu, D.-T.; Chukwu, I. S.; Dadras, O.; Dagnaw, F. T.; Dai, X.; Das, S.; Dastiridou, A.; Debela, S. A.; Demisse, F. W.; Demissie, S.; Dereje, D.; Derese, M.; Desai, H. D.; Dessalegn, F. N.; Dessalegni, S. A. A.; Desye, B.; Dhaduk, K.; Dhimal, M.; Dhingra, S.; Diao, N.; Diaz, D.; Djalalinia, S.; Dodangeh, M.; Dongarwar, D.; Dora, B. T.; Dorostkar, F.; Dsouza, H. L.; Dubljanin, E.; Dunachie, S. J.; Durojaiye, O. C.; Edinur, H. A.; Ejigu, H. B.; Ekholuenetale, M.; Ekundayo, T. C.; El-Abid, H.; Elhadi, M.; Elmonem, M. A.; Emami, A.; Bain, L. E.; Enyew, D. B.; Erkhembayar, R.; Eshrati, B.; Etaee, F.; Fagbamigbe, A. F.; Falahi, S.; Fallahzadeh, A.; Faraon, E. J. A.; Fatehizadeh, A.; Fekadu, G.; Fernandes, J. C.; Ferrari, A.; Fetensa, G.; Filip, I.; Fischer, F.; Foroutan, M.; Gaal, P. A.; Gadanya, M. A.; Gaidhane, A. M.; Ganesan, B.; Gebrehiwot, M.; Ghanbari, R.; Nour, M. G.; Ghashghaee, A.; Gholamrezanezhad, A.; Gholizadeh, A.; Golechha, M.; Goleij, P.; Golinelli, D.; Goodridge, A.; Gunawardane, D. A.; Guo, Y.; Gupta, R. D.; Gupta, S.; Gupta, V. B.; Gupta, V. K.; Guta, A.; Habibzadeh, P.; Avval, A. H.; Halwani, R.; Hanif, A.; Hannan, M. A.; Harapan, H.; Hassan, S.; Hassankhani, H.; Hayat, K.; Heibati, B.; Heidari, G.; Heidari, M.; Heidari-Soureshjani, R.; Herteliu, C.; Heyi, D. Z.; Hezam, K.; Hoogar, P.; Horita, N.; Hossain, M. M.; Hosseinzadeh, M.; Hostiuc, M.; Hostiuc, S.; Hoveidamanesh, S.; Huang, J.; Hussain, S.; Hussein, N. R.; Ibitoye, S. E.; Ilesanmi, O. S.; Ilic, I. M.; Ilic, M. D.; Imam, M. T.; Immurana, M.; Inbaraj, L. R.; Iradukunda, A.; Ismail, N. E.; Iwu, C. C. D.; Iwu, C. J.; J, L. M.; Jakovljevic, M.; Jamshidi, E.; Javaheri, T.; Javanmardi, F.; Javidnia, J.; Jayapal, S. K.; Jayarajah, U.; Jebai, R.; Jha, R. P.; Joo, T.; Joseph, N.; Joukar, F.; Jozwiak, J. J.; Kacimi, S. E. O.; Kadashetti, V.; Kalankesh, L. R.; Kalhor, R.; Kamal, V. K.; Kandel, H.; Kapoor, N.; Karkhah, S.; Kassa, B. G.; Kassebaum, N. J.; Katoto, P. D.; Keykhaei, M.; Khajuria, H.; Khan, A.; Khan, I. A.; Khan, M.; Khan, M. N.; Khan, M. A.; Khatatbeh, M. M.; Khater, M. M.; Kashani, H. R. K.; Khubchandani, J.; Kim, H.; Kim, M. S.; Kimokoti, R. W.; Kissoon, N.; Kochhar, S.; Kompani, F.; Kosen, S.; Koul, P. A.; Laxminarayana, S. L. K.; Lopez, F. K.; Krishan, K.; Krishnamoorthy, V.; Kulkarni, V.; Kumar, N.; Kurmi, O. P.; Kuttikkattu, A.; Kyu, H. H.; Lal, D. K.; Lám, J.; Landires, I.; Lasrado, S.; Lee, S.; Lenzi, J.; Lewycka, S.; Li, S.; Lim, S. S.; Liu, W.; Lodha, R.; Loftus, M. J.; Lohiya, A.; Lorenzovici, L.; Lotfi, M.; Mahmoodpoor, A.; Mahmoud, M. A.; Mahmoudi, R.; Majeed, A.; Majidpoor, J.; Makki, A.; Mamo, G. A.; Manla, Y.; Martorell, M.; Matei, C. N.; McManigal, B.; Nasab, E. M.; Mehrotra, R.; Melese, A.; Mendoza-Cano, O.; Menezes, R. G.; Mentis, A.-F. A.; Micha, G.; Michalek, I. M.; Sá, A. C. M. G. N. de; Kostova, N. M.; Mir, S. A.; Mirghafourvand, M.; Mirmoeeni, S.; Mirrakhimov, E. M.; Mirza-Aghazadeh-Attari, M.; Misganaw, A. S.; Misganaw, A.; Misra, S.; Mohammadi, E.; Mohammadi, M.; Mohammadian-Hafshejani, A.; Mohammed, S.; Mohan, S.; Mohseni, M.; Mokdad, A. H.; Momtazmanesh, S.; Monasta, L.; Moore, C. E.; Moradi, M.; Sarabi, M. M.; Morrison, S. D.; Motaghinejad, M.; Isfahani, H. M.; Khaneghah, A. M.; Mousavi-Aghdas, S. A.; Mubarik, S.; Mulita, F.; Mulu, G. B. B.; Munro, S. B.; Muthupandian, S.; Nair, T. S.; Naqvi, A. A.; Narang, H.; Natto, Z. S.; Naveed, M.; Nayak, B. P.; Naz, S.; Negoi, I.; Nejadghaderi, S. A.; Kandel, S. N.; Ngwa, C. H.; Niazi, R. K.; Sá, A. T. N. de; Noroozi, N.; Nouraei, H.; Nowroozi, A.; Nuñez-Samudio, V.; Nutor, J. J.; Nzoputam, C. I.; Nzoputam, O. J.; Oancea, B.; Obaidur, R. M.; Ojha, V. A.; Okekunle, A. P.; Okonji, O. C.; Olagunju, A. T.; Olusanya, B. O.; Bali, A. O.; Omer, E.; Otstavnov, N.; Oumer, B.; A, M. P.; Padubidri, J. R.; Pakshir, K.; Palicz, T.; Pana, A.; Pardhan, S.; Paredes, J. L.; Parekh, U.; Park, E.-C.; Park, S.; Pathak, A.; Paudel, R.; Paudel, U.; Pawar, S.; Toroudi, H. P.; Peng, M.; Pensato, U.; Pepito, V. C. F.; Pereira, M.; Peres, M. F. P.; Perico, N.; Petcu, I.-R.; Piracha, Z. Z.; Podder, I.; Pokhrel, N.; Poluru, R.; Postma, M. J.; Pourtaheri, N.; Prashant, A.; Qattea, I.; Rabiee, M.; Rabiee, N.; Radfar, A.; Raeghi, S.; Rafiei, S.; Raghav, P. R.; Rahbarnia, L.; Rahimi-Movaghar, V.; Rahman, M.; Rahman, M. A.; Rahmani, A. M.;

Rahmanian, V.; Ram, P.; Ranjha, M. M. A. N.; Rao, S. J.; Rashidi, M.-M.; Rasul, A.; Ratan, Z. A.; Rawaf, S.; Rawassizadeh, R.; Razeghinia, M. S.; Redwan, E. M. M.; Regasa, M. T.; Remuzzi, G.; Reta, M. A.; Rezaei, N.; Rezapour, A.; Riad, A.; Ripon, R. K.; Rudd, K. E.; Saddik, B.; Sadeghian, S.; Saeed, U.; Safaei, M.; Safary, A.; Safi, S. Z.; Sahebazzamani, M.; Sahebkar, A.; Sahoo, H.; Salahi, S.; Salahi, S.; Salari, H.; Salehi, S.; Kafil, H. S.; Samy, A. M.; Sanadgol, N.; Sankararaman, S.; Sanmarchi, F.; Sathian, B.; Sawhney, M.; Saya, G. K.; Senthilkumaran, S.; Seylani, A.; Shah, P. A.; Shaikh, M. A.; Shaker, E.; Shakhmardanov, M. Z.; Sharew, M. M.; Sharifi-Razavi, A.; Sharma, P.; Sheikhi, R. A.; Sheikhy, A.; Shetty, P. H.; Shigematsu, M.; Shin, J. I.; Shirzad-Aski, H.; Shivakumar, K. M.; Shobeiri, P.; Shorofi, S. A.; Shrestha, S.; Sibhat, M. M.; Sidemo, N. B.; Sikder, M. K.; Silva, L. M. L. R.; Singh, J. A.; Singh, P.; Singh, S.; Siraj, M. S.; Siwal, S. S.; Skryabin, V. Y.; Skryabina, A. A.; Socea, B.; Solomon, D. D.; Song, Y.; Sreeramareddy, C. T.; Suleman, M.; Abdulkader, R. S.; Sultana, S.; Szócska, M.; Tabatabaeizadeh, S.-A.; Tabish, M.; Taheri, M.; Taki, E.; Tan, K.-K.; Tandukar, S.; Tat, N. Y.; Tat, V. Y.; Tefera, B. N.; Tefera, Y. M.; Temesgen, G.; Temsah, M.-H.; Tharwat, S.; Thiyagarajan, A.; Tleyjeh, I. I.; Troeger, C. E.; Umapathi, K. K.; Upadhyay, E.; Tahbaz, S. V.; Valdez, P. R.; Eynde, J. V. den; Doorn, H. R. van; Vaziri, S.; Verras, G.-I.; Viswanathan, H.; Vo, B.; Waris, A.; Wassie, G. T.; Wickramasinghe, N. D.; Yaghoubi, S.; Yahya, G. A. T. Y.; Jabbari, S. H. Y.; Yigit, A.; Yiğit, V.; Yon, D. K.; Yonemoto, N.; Zahir, M.; Zaman, B. A.; Zaman, S. B.; Zangiabadian, M.; Zare, I.; Zastrozhin, M. S.; Zhang, Z.-J.; Zheng, P.; Zhong, C.; Zoladl, M.; Zumla, A.; Hay, S. I.; Dolecek, C.; Sartorius, B.; Murray, C. J. L.; Naghavi, M. Global Mortality Associated with 33 Bacterial Pathogens in 2019: A Systematic Analysis for the Global Burden of Disease Study 2019. *The Lancet* **2022**, *400* (10369), 2221–2248. https://doi.org/10.1016/S0140-6736(22)02185-7.

(2) Larsson, D. G. J.; Flach, C.-F. Antibiotic Resistance in the Environment. *Nat Rev Microbiol* **2022**, *20* (5), 257–269. https://doi.org/10.1038/s41579-021-00649-x.

(3) Huemer, M.; Mairpady Shambat, S.; Brugger, S. D.; Zinkernagel, A. S. Antibiotic Resistance and Persistence—Implications for Human Health and Treatment Perspectives. *EMBO reports* **2020**, *21* (12), e51034. https://doi.org/10.15252/embr.202051034.

(4) Aslam, B.; Wang, W.; Arshad, M. I.; Khurshid, M.; Muzammil, S.; Rasool, M. H.; Nisar, M. A.; Alvi, R. F.; Aslam, M. A.; Qamar, M. U.; Salamat, M. K. F.; Baloch, Z. Antibiotic Resistance: A Rundown of a Global Crisis. *Infection and Drug Resistance* **2018**, *11*, 1645–1658. https://doi.org/10.2147/IDR.S173867.

(5) Silhavy, T. J.; Kahne, D.; Walker, S. The Bacterial Cell Envelope. *Cold Spring Harb Perspect Biol* **2010**, *2* (5), a000414. https://doi.org/10.1101/cshperspect.a000414.

(6) Henderson, J. C.; Zimmerman, S. M.; Crofts, A. A.; Boll, J. M.; Kuhns, L. G.; Herrera, C. M.; Trent, M. S. The Power of Asymmetry: Architecture and Assembly of the Gram-Negative Outer Membrane Lipid Bilayer. *Annual Review of Microbiology* **2016**, *70* (1), 255–278. https://doi.org/10.1146/annurev-micro-102215-095308.

(7) Simpson, B. W.; Trent, M. S. Pushing the Envelope: LPS Modifications and Their Consequences. *Nat Rev Microbiol* **2019**, *17* (7), 403–416. https://doi.org/10.1038/s41579-019-0201-x.

(8) Okuda, S.; Sherman, D. J.; Silhavy, T. J.; Ruiz, N.; Kahne, D. Lipopolysaccharide Transport and Assembly at the Outer Membrane: The PEZ Model. *Nat Rev Microbiol* **2016**, *14* (6), 337–345. https://doi.org/10.1038/nrmicro.2016.25.

(9) Malinverni, J. C.; Silhavy, T. J. An ABC Transport System That Maintains Lipid Asymmetry in the Gram-Negative Outer Membrane. *Proceedings of the National Academy of Sciences* **2009**, *106* (19), 8009–8014. https://doi.org/10.1073/pnas.0903229106.

(10) Powers, M. J.; Trent, M. S. Intermembrane Transport: Glycerophospholipid Homeostasis of the Gram-Negative Cell Envelope. *Proceedings of the National Academy of Sciences* **2019**, *116* (35), 17147–17155. https://doi.org/10.1073/pnas.1902026116.

(11) Abellón-Ruiz, J.; Kaptan, S. S.; Baslé, A.; Claudi, B.; Bumann, D.; Kleinekathöfer, U.; van den Berg, B. Structural Basis for Maintenance of Bacterial Outer Membrane Lipid Asymmetry. *Nat Microbiol* **2017**, *2* (12), 1616–1623. https://doi.org/10.1038/s41564-017-0046-x.
(12) Huang, Y. M.; Miao, Y.; Munguia, J.; Lin, L.; Nizet, V.; McCammon, J. A. Molecular Dynamic Study of MlaC Protein in Gram-Negative Bacteria: Conformational Flexibility, Solvent Effect and Protein-Phospholipid Binding. *Protein Science* **2016**, *25* (8), 1430–1437. https://doi.org/10.1002/pro.2939.
(13) Thong, S.; Ercan, B.; Torta, F.; Fong, Z. Y.; Wong, H. Y. A.; Wenk, M. R.; Chng, S.-S. Defining Key Roles for Auxiliary Proteins in an ABC Transporter That Maintains Bacterial Outer Membrane Lipid Asymmetry. *eLife* **2016**, *5*, e19042. https://doi.org/10.7554/eLife.19042.
(14) Ekiert, D. C.; Coudray, N.; Bhabha, G. Structure and Mechanism of the Bacterial Lipid ABC Transporter, MlaFEDB. *Current Opinion in Structural Biology* **2022**, *76*, 102429. https://doi.org/10.1016/j.sbi.2022.102429.
(15) Zhou, C.; Shi, H.; Zhang, M.; Zhou, L.; Xiao, L.; Feng, S.; Im, W.; Zhou, M.; Zhang, X.; Huang, Y. Structural Insight into Phospholipid Transport by the MlaFEBD Complex from P. Aeruginosa. *Journal of Molecular Biology* **2021**, *433* (13), 166986. https://doi.org/10.1016/j.jmb.2021.166986.
(16) Kamischke, C.; Fan, J.; Bergeron, J.; Kulasekara, H. D.; Dalebroux, Z. D.; Burrell, A.; Kollman, J. M.; Miller, S. I. The Acinetobacter Baumannii Mla System and Glycerophospholipid Transport to the Outer Membrane. *eLife* **2019**, *8*, e40171. https://doi.org/10.7554/eLife.40171.
(17) Hughes, G. W.; Hall, S. C. L.; Laxton, C. S.; Sridhar, P.; Mahadi, A. H.; Hatton, C.; Piggot, T. J.; Wotherspoon, P. J.; Leney, A. C.; Ward, D. G.; Jamshad, M.; Spana, V.; Cadby, I. T.; Harding, C.; Isom, G. L.; Bryant, J. A.; Parr, R. J.; Yakub, Y.; Jeeves, M.; Huber, D.; Henderson, I. R.; Clifton, L. A.; Lovering, A. L.; Knowles, T. J. Evidence for Phospholipid Export from the Bacterial Inner Membrane by the Mla ABC Transport System. *Nat Microbiol* **2019**, *4* (10), 1692–1705. https://doi.org/10.1038/s41564-019-0481-y.
(18) Sutterlin, H. A.; Shi, H.; May, K. L.; Miguel, A.; Khare, S.; Huang, K. C.; Silhavy, T. J. Disruption of Lipid Homeostasis in the Gram-Negative Cell Envelope Activates a Novel Cell Death Pathway. *Proceedings of the National Academy of Sciences* **2016**, *113* (11), E1565–E1574. https://doi.org/10.1073/pnas.1601375113.
(19) Chong, Z.-S.; Woo, W.-F.; Chng, S.-S. Osmoporin OmpC Forms a Complex with MlaA to Maintain Outer Membrane Lipid Asymmetry in Escherichia Coli. *Molecular Microbiology* **2015**, *98* (6), 1133–1146. https://doi.org/10.1111/mmi.13202.
(20) Baarda, B. I.; Zielke, R. A.; Van, A. L.; Jerse, A. E.; Sikora, A. E. Neisseria Gonorrhoeae MlaA Influences Gonococcal Virulence and Membrane Vesicle Production. *PLOS Pathogens* **2019**, *15* (3), e1007385. https://doi.org/10.1371/journal.ppat.1007385.
(21) Powers, M. J.; Trent, M. S. Phospholipid Retention in the Absence of Asymmetry Strengthens the Outer Membrane Permeability Barrier to Last-Resort Antibiotics. *Proceedings of the National Academy of Sciences* **2018**, *115* (36), E8518–E8527. https://doi.org/10.1073/pnas.1806714115.
(22) Powers, M. J.; Simpson, B. W.; Trent, M. S. The Mla Pathway in Acinetobacter Baumannii Has No Demonstrable Role in Anterograde Lipid Transport. *eLife* **2020**, *9*, e56571. https://doi.org/10.7554/eLife.56571.
(23) Low, W.-Y.; Chng, S.-S. Current Mechanistic Understanding of Intermembrane Lipid Trafficking Important for Maintenance of Bacterial Outer Membrane Lipid Asymmetry. *Current Opinion in Chemical Biology* **2021**, *65*, 163–171. https://doi.org/10.1016/j.cbpa.2021.09.004.
(24) Nagy, E.; Losick, R.; Kahne, D. Robust Suppression of Lipopolysaccharide Deficiency in Acinetobacter Baumannii by Growth in Minimal Medium. *Journal of Bacteriology* **2019**, *201* (22), 10.1128/jb.00420-19. https://doi.org/10.1128/jb.00420-19.

(25) Yeow, J.; Luo, M.; Chng, S.-S. Molecular Mechanism of Phospholipid Transport at the Bacterial Outer Membrane Interface. *Nat Commun* **2023**, *14* (1), 8285. https://doi.org/10.1038/s41467-023-44144-8.
(26) Yero, D.; Díaz-Lobo, M.; Costenaro, L.; Conchillo-Solé, O.; Mayo, A.; Ferrer-Navarro, M.; Vilaseca, M.; Gibert, I.; Daura, X. The Pseudomonas Aeruginosa Substrate-Binding Protein Ttg2D Functions as a General Glycerophospholipid Transporter across the Periplasm. *Commun Biol* **2021**, *4* (1), 1–16. https://doi.org/10.1038/s42003-021-01968-8.
(27) Dutta, A.; Prasad Kanaujia, S. MlaC Belongs to a Unique Class of Non-Canonical Substrate-Binding Proteins and Follows a Novel Phospholipid-Binding Mechanism. *Journal of Structural Biology* **2022**, *214* (4), 107896. https://doi.org/10.1016/j.jsb.2022.107896.
(28) MacRae, M. R.; Puvanendran, D.; Haase, M. A. B.; Coudray, N.; Kolich, L.; Lam, C.; Baek, M.; Bhabha, G.; Ekiert, D. C. Protein-Protein Interactions in the Mla Lipid Transport System Probed by Computational Structure Prediction and Deep Mutational Scanning. *Journal of Biological Chemistry* **2023**, 104744. https://doi.org/10.1016/j.jbc.2023.104744.
(29) Agasid, M. T.; Robinson, C. V. Probing Membrane Protein–Lipid Interactions. *Current Opinion in Structural Biology* **2021**, *69*, 78–85. https://doi.org/10.1016/j.sbi.2021.03.010.
(30) Bolla, J. R.; Agasid, M. T.; Mehmood, S.; Robinson, C. V. Membrane Protein–Lipid Interactions Probed Using Mass Spectrometry. *Annual Review of Biochemistry* **2019**, *88* (1), 85–111. https://doi.org/10.1146/annurev-biochem-013118-111508.
(31) Ekiert, D. C.; Bhabha, G.; Isom, G. L.; Greenan, G.; Ovchinnikov, S.; Henderson, I. R.; Cox, J. S.; Vale, R. D. Architectures of Lipid Transport Systems for the Bacterial Outer Membrane. *Cell* **2017**, *169* (2), 273-285.e17. https://doi.org/10.1016/j.cell.2017.03.019.
(32) Karch, K. R.; Snyder, D. T.; Harvey, S. R.; Wysocki, V. H. Native Mass Spectrometry: Recent Progress and Remaining Challenges. *Annual Review of Biophysics* **2022**, *51* (1), 157–179. https://doi.org/10.1146/annurev-biophys-092721-085421.
(33) Barth, M.; Schmidt, C. Native Mass Spectrometry—A Valuable Tool in Structural Biology. *Journal of Mass Spectrometry* **2020**, *55* (10), e4578. https://doi.org/10.1002/jms.4578.
(34) Lee, T.-H.; Hofferek, V.; Separovic, F.; Reid, G. E.; Aguilar, M.-I. The Role of Bacterial Lipid Diversity and Membrane Properties in Modulating Antimicrobial Peptide Activity and Drug Resistance. *Current Opinion in Chemical Biology* **2019**, *52*, 85–92. https://doi.org/10.1016/j.cbpa.2019.05.025.
(35) Cramer, D. A. T.; Franc, V.; Caval, T.; Heck, A. J. R. Charting the Proteoform Landscape of Serum Proteins in Individual Donors by High-Resolution Native Mass Spectrometry. *Anal. Chem.* **2022**, *94* (37), 12732–12741. https://doi.org/10.1021/acs.analchem.2c02215.
(36) Sipe, S. N.; Patrick, J. W.; Laganowsky, A.; Brodbelt, J. S. Enhanced Characterization of Membrane Protein Complexes by Ultraviolet Photodissociation Mass Spectrometry. *Anal. Chem.* **2020**, *92* (1), 899–907. https://doi.org/10.1021/acs.analchem.9b03689.
(37) O'Brien, J. P.; Li, W.; Zhang, Y.; Brodbelt, J. S. Characterization of Native Protein Complexes Using Ultraviolet Photodissociation Mass Spectrometry. *J. Am. Chem. Soc.* **2014**, *136* (37), 12920–12928. https://doi.org/10.1021/ja505217w.
(38) Cammarata, M. B.; Brodbelt, J. S. Structural Characterization of Holo- and Apo-Myoglobin in the Gas Phase by Ultraviolet Photodissociation Mass Spectrometry. *Chem. Sci.* **2015**, *6* (2), 1324–1333. https://doi.org/10.1039/C4SC03200D.
(39) Mehaffey, M. R.; Cammarata, M. B.; Brodbelt, J. S. Tracking the Catalytic Cycle of Adenylate Kinase by Ultraviolet Photodissociation Mass Spectrometry. *Anal. Chem.* **2018**, *90* (1), 839–846. https://doi.org/10.1021/acs.analchem.7b03591.
(40) Blevins, M. S.; James, V. K.; Herrera, C. M.; Purcell, A. B.; Trent, M. S.; Brodbelt, J. S. Unsaturation Elements and Other Modifications of Phospholipids in Bacteria: New Insight from Ultraviolet

Photodissociation Mass Spectrometry. *Anal. Chem.* **2020**, *92* (13), 9146–9155. https://doi.org/10.1021/acs.analchem.0c01449.
(41) Blevins, M. S.; Shields, S. W. J.; Cui, W.; Fallatah, W.; Moser, A. B.; Braverman, N. E.; Brodbelt, J. S. Structural Characterization and Quantitation of Ether-Linked Glycerophospholipids in Peroxisome Biogenesis Disorder Tissue by Ultraviolet Photodissociation Mass Spectrometry. *Anal. Chem.* **2022**, *94* (37), 12621–12629. https://doi.org/10.1021/acs.analchem.2c01274.
(42) Cong, X.; Liu, Y.; Liu, W.; Liang, X.; Russell, D. H.; Laganowsky, A. Determining Membrane Protein–Lipid Binding Thermodynamics Using Native Mass Spectrometry. *J. Am. Chem. Soc.* **2016**, *138* (13), 4346–4349. https://doi.org/10.1021/jacs.6b01771.
(43) Lyu, J.; Zhang, T.; Marty, M. T.; Clemmer, D.; Russell, D. H.; Laganowsky, A. Double and Triple Thermodynamic Mutant Cycles Reveal the Basis for Specific MsbA-Lipid Interactions. *eLife* **2024**, *12*. https://doi.org/10.7554/eLife.91094.2.
(44) Laganowsky, A.; Reading, E.; Allison, T. M.; Ulmschneider, M. B.; Degiacomi, M. T.; Baldwin, A. J.; Robinson, C. V. Membrane Proteins Bind Lipids Selectively to Modulate Their Structure and Function. *Nature* **2014**, *510* (7503), 172–175. https://doi.org/10.1038/nature13419.
(45) Liu, Y.; Cong, X.; Liu, W.; Laganowsky, A. Characterization of Membrane Protein–Lipid Interactions by Mass Spectrometry Ion Mobility Mass Spectrometry. *J. Am. Soc. Mass Spectrom.* **2017**, *28* (4), 579–586. https://doi.org/10.1007/s13361-016-1555-1.
(46) Laganowsky, A.; Reading, E.; Hopper, J. T. S.; Robinson, C. V. Mass Spectrometry of Intact Membrane Protein Complexes. *Nat Protoc* **2013**, *8* (4), 639–651. https://doi.org/10.1038/nprot.2013.024.
(47) Zhang, G.; Odenkirk, M. T.; Janczak, C. M.; Lee, R.; Richardson, K.; Wang, Z.; Aspinwall, C. A.; Marty, M. T. Identifying Membrane Protein–Lipid Interactions with Lipidomic Lipid Exchange-Mass Spectrometry. *J. Am. Chem. Soc.* **2023**, *145* (38), 20859–20867. https://doi.org/10.1021/jacs.3c05883.
(48) Keener, J. E.; Jayasekera, H. S.; Marty, M. T. Investigating the Lipid Selectivity of Membrane Proteins in Heterogeneous Nanodiscs. *Anal. Chem.* **2022**, *94* (23), 8497–8505. https://doi.org/10.1021/acs.analchem.2c01488.
(49) Sanders, J. D.; Shields, S. W.; Escobar, E. E.; Lanzillotti, M. B.; Butalewicz, J. P.; James, V. K.; Blevins, M. S.; Sipe, S. N.; Brodbelt, J. S. Enhanced Ion Mobility Separation and Characterization of Isomeric Phosphatidylcholines Using Absorption Mode Fourier Transform Multiplexing and Ultraviolet Photodissociation Mass Spectrometry. *Anal. Chem.* **2022**, *94* (10), 4252–4259. https://doi.org/10.1021/acs.analchem.1c04711.
(50) Blevins, M. S.; Juetten, K. J.; James, V. K.; Butalewicz, J. P.; Escobar, E. E.; Lanzillotti, M. B.; Sanders, J. D.; Fort, K. L.; Brodbelt, J. S. Nanohydrophobic Interaction Chromatography Coupled to Ultraviolet Photodissociation Mass Spectrometry for the Analysis of Intact Proteins in Low Charge States. *J. Proteome Res.* **2022**, *21* (10), 2493–2503. https://doi.org/10.1021/acs.jproteome.2c00450.
(51) Sipe, S. N.; Lancaster, E. B.; Butalewicz, J. P.; Whitman, C. P.; Brodbelt, J. S. Symmetry of 4-Oxalocrotonate Tautomerase Trimers Influences Unfolding and Fragmentation in the Gas Phase. *J. Am. Chem. Soc.* **2022**, *144* (27), 12299–12309. https://doi.org/10.1021/jacs.2c03564.
(52) McCabe, J. W.; Shirzadeh, M.; Walker, T. E.; Lin, C.-W.; Jones, B. J.; Wysocki, V. H.; Barondeau, D. P.; Clemmer, D. E.; Laganowsky, A.; Russell, D. H. Variable-Temperature Electrospray Ionization for Temperature-Dependent Folding/Refolding Reactions of Proteins and Ligand Binding. *Anal. Chem.* **2021**, *93* (18), 6924–6931. https://doi.org/10.1021/acs.analchem.1c00870.
(53) Sanders, J. D.; Grinfeld, D.; Aizikov, K.; Makarov, A.; Holden, D. D.; Brodbelt, J. S. Determination of Collision Cross-Sections of Protein Ions in an Orbitrap Mass Analyzer. *Anal. Chem.* **2018**, *90* (9), 5896–5902. https://doi.org/10.1021/acs.analchem.8b00724.

(54) James, V. K.; Sanders, J. D.; Aizikov, K.; Fort, K. L.; Grinfeld, D.; Makarov, A.; Brodbelt, J. S. Advancing Orbitrap Measurements of Collision Cross Sections to Multiple Species for Broad Applications. *Anal. Chem.* **2022**, *94* (45), 15613–15620. https://doi.org/10.1021/acs.analchem.2c02146.
(55) James, V. K.; Sanders, J. D.; Aizikov, K.; Fort, K. L.; Grinfeld, D.; Makarov, A.; Brodbelt, J. S. Expanding Orbitrap Collision Cross-Section Measurements to Native Protein Applications Through Kinetic Energy and Signal Decay Analysis. *Anal. Chem.* **2023**, *95* (19), 7656–7664. https://doi.org/10.1021/acs.analchem.3c00594.
(56) Juetten, K. J.; Brodbelt, J. S. MS-TAFI: A Tool for the Analysis of Fragment Ions Generated from Intact Proteins. *J. Proteome Res.* **2023**, *22* (2), 546–550. https://doi.org/10.1021/acs.jproteome.2c00594.
(57) Durbin, K. R.; Robey, M. T.; Voong, L. N.; Fellers, R. T.; Lutomski, C. A.; El-Baba, T. J.; Robinson, C. V.; Kelleher, N. L. ProSight Native: Defining Protein Complex Composition from Native Top-Down Mass Spectrometry Data. *J. Proteome Res.* **2023**, *22* (8), 2660–2668. https://doi.org/10.1021/acs.jproteome.3c00171.
(58) Marty, M. T.; Baldwin, A. J.; Marklund, E. G.; Hochberg, G. K. A.; Benesch, J. L. P.; Robinson, C. V. Bayesian Deconvolution of Mass and Ion Mobility Spectra: From Binary Interactions to Polydisperse Ensembles. *Anal. Chem.* **2015**, *87* (8), 4370–4376. https://doi.org/10.1021/acs.analchem.5b00140.
(59) Kostelic, M. M.; Marty, M. T. Deconvolving Native and Intact Protein Mass Spectra with UniDec. In *Proteoform Identification: Methods and Protocols*; Sun, L., Liu, X., Eds.; Methods in Molecular Biology; Springer US: New York, NY, 2022; pp 159–180. https://doi.org/10.1007/978-1-0716-2325-1_12.
(60) Arechaga, I.; Miroux, B.; Karrasch, S.; Huijbregts, R.; de Kruijff, B.; Runswick, M. J.; Walker, J. E. Characterisation of New Intracellular Membranes in Escherichia Coli Accompanying Large Scale Over-Production of the b Subunit of F1Fo ATP Synthase. *FEBS Letters* **2000**, *482* (3), 215–219. https://doi.org/10.1016/S0014-5793(00)02054-8.
(61) Kwon, Y.-C.; Jewett, M. C. High-Throughput Preparation Methods of Crude Extract for Robust Cell-Free Protein Synthesis. *Sci Rep* **2015**, *5* (1), 8663. https://doi.org/10.1038/srep08663.
(62) Gupta, K.; Li, J.; Liko, I.; Gault, J.; Bechara, C.; Wu, D.; Hopper, J. T. S.; Giles, K.; Benesch, J. L. P.; Robinson, C. V. Identifying Key Membrane Protein Lipid Interactions Using Mass Spectrometry. *Nat Protoc* **2018**, *13* (5), 1106–1120. https://doi.org/10.1038/nprot.2018.014.
(63) Ambrose, S.; Housden, N. G.; Gupta, K.; Fan, J.; White, P.; Yen, H.-Y.; Marcoux, J.; Kleanthous, C.; Hopper, J. T. S.; Robinson, C. V. Native Desorption Electrospray Ionization Liberates Soluble and Membrane Protein Complexes from Surfaces. *Angewandte Chemie* **2017**, *129* (46), 14655–14660. https://doi.org/10.1002/ange.201704849.

TOC